Chiral protein scissors: High enantiomeric selectivity for binding and its effect on protein photocleavage efficiency and specificity

Challa V. Kumar*†, Apinya Buranaprapuk†‡, Ho C. Sze†, Steffen Jockusch§, and Nicholas J. Turro§

†Department of Chemistry, University of Connecticut, U-3060, 55 North Eagleville Road, Storrs, CT 06269-3060; §Department of Chemistry, Columbia University, 3000 Broadway, New York, NY 10027; and ‡Department of Chemistry, Faculty of Science, Srinakarinwirot University, Sukhumvit 23, Bangkok 10110, Thailand

Contributed by Nicholas J. Turro, February 28, 2002

Chiral recognition of protein-binding sites by a simple organic molecule with selectivities >100 is reported here. The L-isomer of 4(1-pyrene)-3-butyroyl-phenylalanine amide (Py-L-Phe) binds to BSA with an affinity constant (K_b) of 3×10^7 M^{-1}, whereas the corresponding D-isomer (Py-D-Phe) binds 100 times weaker. The enantiomers showed contrasting spectral changes when bound to BSA. Whereas hypochromism was observed with the L-isomer, hyperchromism was observed for the D-isomer, and, whereas the fluorescence of the L-isomer was quenched, the fluorescence of the D-isomer was enhanced. The induced CD spectra of the enantiomers bound to BSA bear a near mirror-image relationship. In contrast, the enantiomers show only moderate binding selectivity with lysozyme. The differences in the enantioselectivities with the two proteins indicate that the binding site of 4(1-pyrene)-3-butyroyl-phenylalanine amide (Py-Phe) in BSA is crowded, whereas that of lysozyme is more accommodative of either isomer. The enantioselective binding of Py-Phe isomers is further examined in protein photocleavage studies. Py-D-Phe cleaves BSA and lysozyme at a single site in a manner similar to Py-L-Phe, but the cleavage yields are lower for the D-isomer. Sequencing of the resulting fragments indicated that the photocleavage sites of Py-D-Phe on BSA and lysozyme are identical to those of Py-L-Phe. Flash photolysis studies indicated only minor differences between the two enantiomers. The large binding selectivities, therefore, do not influence cleavage specificity or cleavage site location. The strong role of the single asymmetric center of Py-Phe in recognition and its minor role in photocleavage chemistry are demonstrated.

The development of photochemical reagents to cleave proteins with a high specificity is of intense interest because of their potential for applications in molecular biology, as well as for understanding biomolecular recognition with small ligands (1–2). Because of the extreme stability of the peptide bond (half life of ≈7 years at room temperature, pH 7) (3), the development of such reagents is challenging. One approach is to design small organic molecules (probes) that bind to proteins at specific sites with a high affinity and to use these chromophores to sensitize the photogeneration of reactive intermediates for protein cleavage (4–8). An examination of a number of enzyme–substrate complexes indicates that chirality of the ligand is an important feature in the recognition of the binding site on a protein (9), and hence the introduction of asymmetric centers at specific sites on a probe is a convenient handle to control recognition by photocleavage reagents (10). Even though the enantioselective binding of substrates to enzymes and other biomacromolecules is well known, designing small organic molecules with high enantioselectivity for specific protein targets has been challenging (11).

Binding of dansyl amino acids, drugs, and metal complexes to BSA, chymotrypsin, and other proteins results in only moderate selectivity (12–16), and enantioselective binding of metal complexes to DNA is well documented (17). Such chiral host systems are useful in separating the optical isomers of drugs, amino acids, metal complexes, and other organic molecules, indicating the utility of such recognition in chiral applications (12–16). In most of these examples, the enantioselective binding of ligands to the target biomolecule is moderate, and the ratio of the binding constants of the enantiomers has been in the range 1.15–3 (12–16). The observed enantiomeric selectivity, however, was explained on the basis of steric, hydrophobic, and hydrogen-bonding interactions between the ligand and the host, resulting in a tight fitting of the probe within the three-dimensional space of the host cavity (18). Designing nonnatural ligands that bind to proteins with a high enantiomeric selectivity (>10), therefore, is challenging. Such an effort will help in understanding the role of chirality in biomolecular recognition and is central to the design of reagents targeted to cleave proteins at specific sites (4–8, 10).

Site-specific photocleavage of proteins with high efficiency by using probes based on a pyrenyl chromophore coupled to an asymmetric center was reported recently (4–8, 19). By linking a photoreactive chromophore to natural amino acids or short peptides, protein photocleavage at specific sites was demonstrated. Covalent linking of 4(1-pyrenyl)butyric acid to the N terminus of L-phenylalanine, for example, led to a photoprobe (Py-L-Phe, Scheme 1) that cleaves BSA or lysozyme at a single

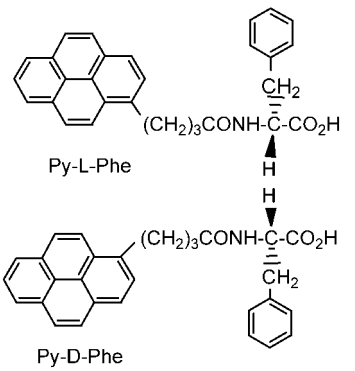

Scheme 1. The chemical structures of the optical isomers of Py-Phe.

site with high quantum efficiency (0.25–0.003) (19). The newly produced photofragments are amenable to sequencing, and BSA was cleaved by Py-L-Phe between Leu-346 and Arg-347. These residues are located in the interior of BSA, near the fatty acid-binding site, in domain II, subdomain C. In contrast,

Abbreviations: Py-Phe, 4(1-pyrene)-3-butyroyl-phenylalanine amide; CoHA, hexammineCo(III) chloride.

*To whom reprint requests should be addressed. E-mail: c.v.kumar@uconn.edu.

The publication costs of this article were defrayed in part by page charge payment. This article must therefore be hereby marked "*advertisement*" in accordance with 18 U.S.C. §1734 solely to indicate this fact.

www.pnas.org/cgi/doi/10.1073/pnas.082119599

lysozyme was cleaved at a site exposed to the solvent, between Trp-108 and Val-109, away from the catalytic site. In addition to cleaving at a single site, the photoreaction did not alter the enzymatic activity of lysozyme, indicating the gentle nature of the cleavage chemistry toward the sensitive residues at the catalytic site (19). Control over the location of the photocleavage site was demonstrated when additional residues were inserted between the pyrenyl chromophore and phenylalanine of 4(1-pyrene)-3-butyroyl-phenylalanine amide (Py-Phe) (20). In these cases, the photocleavage was observed at sites that are further away from the Py-L-Phe cleavage site, and the distance of separation between the chromophore and Phe residue is important in determining the location of the photocleavage site.

The specificity of the protein photocleavage was attributed to the tight binding of Py-L-Phe at residues 346–347 in BSA and residues 108–109 in lysozyme such that the photophore reaches a single site in each of these cases. Such binding is expected to be sensitive to the three-dimensional architecture of the probe, and the single asymmetric center of Py-Phe could play a significant role in binding and recognition. This aspect is now investigated by using the enantiomer, Py-D-Phe, where D-phenylalanine is coupled to the pyrenyl chromophore. The role of the single asymmetric center present in Py-L-Phe in the recognition, as well as the photoreactivity properties of Py-Phe, are reported here.

A strong role of the chiral center in the recognition between the protein and Py-Phe is evident from the binding and photocleavage properties of these enantiomers. If the binding interaction is dominated by the pyrenyl chromophore, then the chiral center will play only a minor role, and the two isomers will have similar binding and cleavage properties. On the other hand, if the phenylalanine part of the probe contributes significantly to the binding interaction, then the chiral center is expected to have a strong influence on binding and possibly on cleavage properties. Preliminary results indicated that the binding constant of Py-L-Phe with BSA is two orders of magnitude greater than the D-isomer, and the protein-bound enantiomers show dramatic differences in their spectral properties (10). These initial studies are confirmed in this report by spectroscopic, photochemical, sequencing, and flash photolysis studies. The similarities and the differences in the properties of the two enantiomers allow us to draw definitive conclusions regarding the role of the chiral center in the recognition and the photocleavage properties.

Materials and Methods

Lysozyme (molecular weight 14,300) and BSA (molecular weight 66,267) (Sigma) solutions were prepared by dissolving appropriate amounts of the protein in 50 mM Tris·HCl buffer, pH 7.0. All solutions were freshly prepared and used on the same day. The absorption spectra were recorded on a Hewlett–Packard Model 8453 diode-array spectrophotometer, and calibration graphs were constructed by using Beer's law. Probe concentrations in our experiments were restricted to the linear region of the calibration graph. The molar extinction coefficients of Py-D-Phe matched with those of Py-L-Phe (33,000 $M^{-1}\cdot cm^{-1}$ at 343 nm) (4–8). The fluorescence spectra were recorded on a Perkin–Elmer LS5 spectrometer interfaced with an Apple Macintosh computer by using software developed in our laboratory. No excimer emission was observed from the probes in the 0–50 μM concentration range. The absorption and fluorescence titrations were performed by keeping the probe concentration constant, while varying the protein concentration under air-saturation conditions. The pyrenyl probe was excited at the corresponding isosbestic point (344/345 nm), and the fluorescence intensity has been monitored at 377 nm as a function of protein concentration.

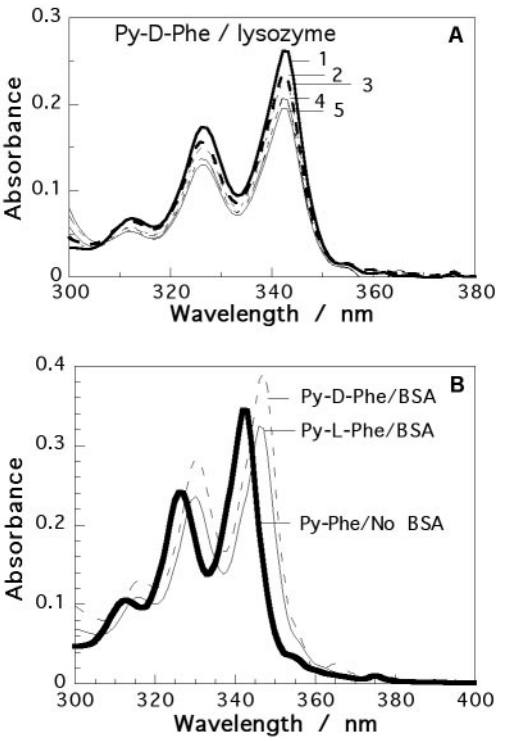

Fig. 1. (*A*) Absorption spectra of Py-D-Phe (10 μM) recorded (1-cm path length) in the presence of increasing concentrations of lysozyme: (1) 0 μM, (2) 4 μM, (3) 6 μM, (4) 8 μM, and (5) 10 μM. (*B*) Absorption spectra of Py-L-Phe or Py-D-Phe (thick line) in the absence of BSA, superimposed on the absorption spectra of Py-D-Phe/BSA (dashed line) and Py-L-Phe/BSA (thin line).

Synthesis of the Probes. Py-D-Phe was synthesized by coupling 4-(1-pyrenyl)butyric acid (1 g) with D-phenylalanine methyl ester (1 g) by using dicyclohexylcarbodiimide (1.2 g), following a procedure similar to that of Py-L-Phe (6). The product was identified to be Py-D-Phe from UV-Vis, fluorescence, CD, NMR, and mass spectral data. ^{1}H NMR (400 MHz, d_6-DMSO): 7.8–8.2 ppm (9H), 7.1 ppm (5H), 4.4 ppm (1H), 3.1 ppm (2H), 1.8–2.1 ppm (6H). MS data (FAB): m/e 436 (MH^+). The absorption, fluorescence, and NMR spectra of the enantiomers are indistinguishable.

Photochemical Protein Cleavage. Protein photocleavage was carried out in 50 mM Tris·HCl buffer, pH 7.0. The protein solution

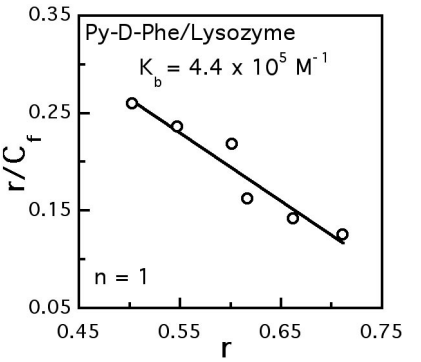

Fig. 2. The binding isotherm constructed from the absorption data shown in Fig. 1*A* for Py-D-Phe/lysozyme, using Scatchard analysis. The line indicates the best linear fit to the data, and the fit indicated a binding constant of 4.4 × $10^5\cdot M^{-1}$ with a single binding site per lysozyme molecule.

Table 1. Binding constants and fluorescence quenching parameters for Py-D-Phe and Py-L-Phe when bound to lysozyme or BSA

Probe/parameter	Py-L-Phe (free)	Py-D-Phe (lysozyme)	Py-L-Phe (lysozyme)	Py-D-Phe (BSA)	Py-L-Phe (BSA)
K_b/M	—	4.4×10^5	2.2×10^5	5.3×10^5	6.7×10^7
K_{SV}/M	1.9×10^3	0.53×10^3	1.4×10^3	—	0.25×10^3

(15 μM), containing Py-D-Phe (15 μM) and $Co(NH_3)_6Cl_3$ (CoHA, 1 mM) (total volume 100 μl) was irradiated at 344 nm (at the pyrenyl absorption band) by using a 150-W xenon lamp attached to a PTI model A1010 monochromator. UV cutoff filter (WG-345; 78%T at 344 nm) was used to remove stray UV light. Samples were withdrawn periodically to test the progress of the photoreaction. Dark control samples were prepared under the same conditions as described above, except that the solutions were protected from light. Protein samples were evaporated under vacuum by using a SpeedVac (Savant, model ISS 110) for gel electrophoresis experiments.

SDS/PAGE. The irradiated samples (100 μl) were dried in a SpeedVac, and the sample was dissolved in the loading buffer (24 μl) containing SDS (7% wt/vol), glycerol (4% wt/vol), Tris (50 mM, pH 6.8), mercaptoethanol (2% vol/vol), and Bromophenol blue (0.01% wt/vol). The protein solutions (8 μl) were denatured by heating to boil for 3 min. The polyacrylamide gel was prepared by following the literature procedure (21), and the samples were loaded for separation. To separate the reaction mixture containing BSA, 8% polyacrylamide (separating) gel was used while the lysozyme reaction mixture was separated by using a 12% polyacrylamide gel. The gel was electrophoresed by applying 60 V until the dye passed into the separating gel, and then the voltage was increased to 100 V. The gels were run for 2 h, stained, and destained as described earlier (19).

Flash Photolysis Studies. Laser flash photolysis experiments used the light pulses (355 nm, ≈8 mJ/pulse, 8 ns) from a Spectra-Physics GCR-150 Nd-YAG laser and a computer-controlled system described elsewhere (22). Kinetic traces were monitored at specific wavelengths, the absorption spectra at various delay times were reconstructed from these traces, and the data were analyzed to extract transient decay kinetics.

Results and Discussion

The role of a single asymmetric center present in Py-Phe on its binding properties and protein photocleavage was examined here. The enantiomers differ in terms of their protein-binding affinities, spectral properties, and protein cleavage. Both isomers cleave the two proteins at identical sites but differ in terms of their yields, despite the differences in their binding behavior.

Absorption Titrations. The electronic absorption spectral features of the pyrenyl chromophore are sensitive to its microenvironment, and the absorption spectra undergo large changes on binding to proteins (23, 24).[¶] Addition of lysozyme (0–10 μM) to a solution of Py-D-Phe (10 μM), for example, results in significant hypochromism (14% at 343 nm, Fig. 1*A*). Such hypochromism is attributed to partial stacking of the aromatic residues of the protein with that of the aromatic pyrenyl chromophore. The absorption peak positions are unchanged, and they indicate a significant exposure of the pyrenyl chromophore to the solvent, in a manner similar to that of Py-L-Phe bound to lysozyme (20). In contrast to this behavior with lysozyme, the binding of Py-D-Phe to BSA results in large red shifts of its absorption peak positions with isosbestic points at 315, 328, and 344 nm and hyperchromism. The absorption spectra of the Py-Phe optical isomers (8.8 μM) in the absence and presence of BSA (10 μM) are compared in Fig. 1*B*. The red shift of the absorption spectra suggests a hydrophobic environment surrounding the pyrenyl chromophore in BSA (23),[¶] in contrast to the analogous binding site in lysozyme. Although the absorption spectra of both the isomers undergo red shifts on binding to BSA, the D-isomer shows hyperchromism, and the L-isomer indicates hypochromism. The pyrenyl absorption bands, therefore, provide a sensitive spectroscopic handle to monitor the subtle differences in the probe environments.

$$r/C_f = K_b\,(n - r) \qquad [1]$$

[¶]Kumar, C. V. & Tolosa, L. M. (1993) *FASEB J.* **7,** A1131 (abstr.).

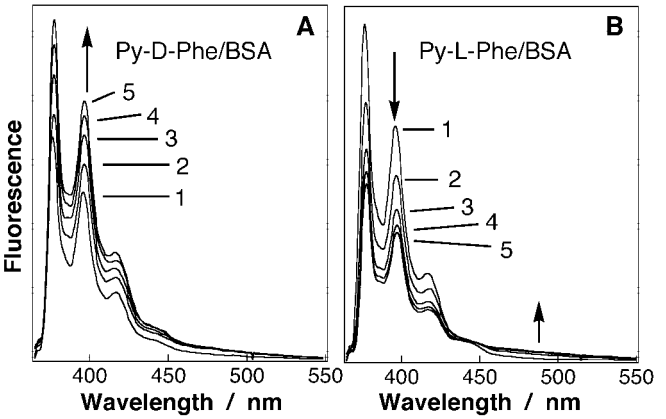

Fig. 3. Fluorescence spectra of Py-D-Phe (2 μM) (*A*) and Py-L-Phe (2 μM) (*B*) in the presence of increasing concentrations of BSA (*A*: spectra 1 through 5 recorded at 0, 2, 4, 6, and 8 μM BSA; *B*: spectra 1–5 recorded at 0, 0.5, 1, 1.5, and 2 μM BSA). The excitation wavelength was at the isosbestic point, 344 nm.

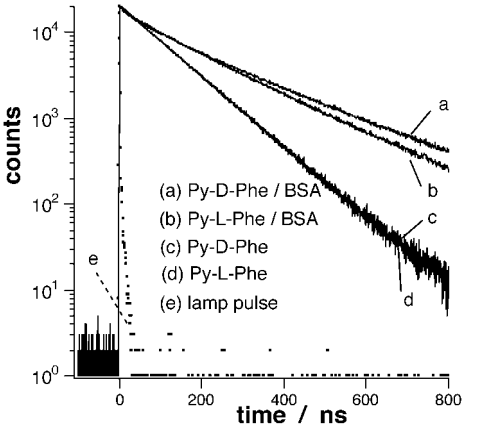

Fig. 4. Fluorescence decay traces of Py-D-Phe (2 μM) and Py-L-Phe (2 μM) in Tris buffer (air-saturated solutions) recorded in the presence of BSA (5 μM, curves a and b) and in the absence of protein (curves c and d). In the absence of the protein (curves c and d), the two decay traces are indistinguishable, whereas in the presence of BSA, the D-isomer indicates a slightly slower decay (curve a) than the L-isomer (curve b). The lamp profile is indicated by the dashed line (curve e).

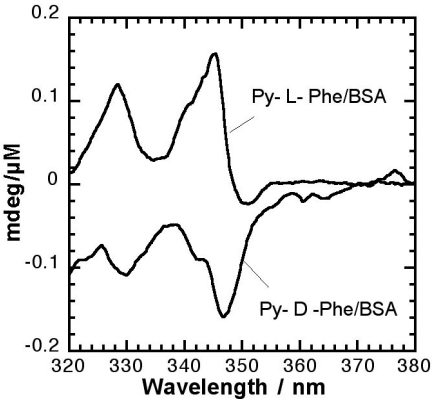

Fig. 5. The induced CD spectra of Py-D-Phe (21 μM) and Py-L-Phe (30 μM) recorded in the presence of BSA (55 μM) (50 mM Tris-HCl, pH 7.0).

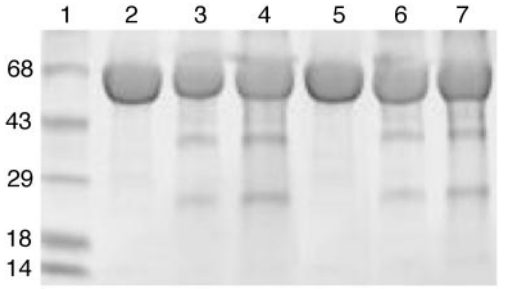

Fig. 7. Site-specific photocleavage of BSA with Py-D-Phe and Py-L-Phe. Lane 1 contains molecular weight markers, as indicated (kDa). Lanes 2–4 contain BSA (15 μM), Py-D-Phe (15 μM), and CoHA (1 mM) that were exposed to 344-nm radiation for 0, 30, and 60 min, respectively. Lanes 5–7 contain BSA (15 μM), Py-L-Phe (15 μM), and CoHA (1 mM) that were exposed to 344-nm radiation for 0, 30, and 60 min, respectively. No photocleavage was observed in the control lanes (lanes 2 and 5).

The absorption spectral data are used to construct the corresponding binding isotherms by using Eq. **1** (25, 26), where r is the number of mols of probe bound per mol of protein, C_f is the free probe concentration, n is number of binding sites per protein, and K_b is the binding constant. A plot of r/C_f as a function of r, for Py-D-Phe binding to lysozyme, is shown in Fig. 2. Analysis of the data indicated a binding constant of $4.4 \pm 0.3 \times 10^5 \cdot M^{-1}$ with a single binding site, and a comparison of this value with the corresponding binding constant of Py-L-Phe/lysozyme ($K_b = 2.2 \pm 0.2 \times 10^5 \cdot M^{-1}$) indicates a chiral selectivity of 2:1. The binding constants of these enantiomers with BSA, obtained in a similar manner, are collected in Table 1. In contrast to the lysozyme data, the D-isomer binds to BSA at least two orders of magnitude weaker than the L-isomer, and the data highlight the differences in the two binding sites. Although the binding site of BSA is rigid, nonpolar, shielded from solvent, and prefers the L-isomer, the binding site of lysozyme is more flexible, polar, and readily accommodates structural variations. In addition to the differences in their selectivities with respect to these proteins, the enantiomers exhibit contrasting behavior in their spectral properties.

Fluorescence Titrations. The fluorescence spectra of Py-D-Phe (2 μM) recorded in the presence of increasing concentrations of lysozyme (0, 2, 4, 6, 8, 10 μM) indicate weak quenching of the pyrenyl fluorescence by the protein (data not shown). The spectral maxima (345-nm excitation) are essentially the same for both isomers, consistent with the above absorption data. In contrast, the optical isomers show large differences in their fluorescence behavior with BSA. The fluorescence intensity of Py-D-Phe (2 μM), for example, is dramatically enhanced by the addition of BSA (0–8 μM, excitation at 345 nm; Fig. 3*A*), whereas that of Py-L-Phe was strongly quenched (Fig. 3*B*). Enhanced fluorescence yields on binding to proteins are generally expected, as in case of Py-D-Phe/BSA, because of the protection of the probe from solvent, oxygen, and other quenchers (23, 24). However, the presence of specific residues at the binding site that function as quenchers such as Trp or Tyr results in strong reduction of probe fluorescence, as in case of Py-L-Phe/BSA (20). Another contrasting feature between the two probes is that no excimer or exciplex emission was observed when Py-D-Phe binds to BSA, whereas Py-L-Phe/BSA shows a long wavelength band at 460 nm (20).

The above scenario predicts longer fluorescence lifetimes for Py-D-Phe/BSA and shorter lifetimes for Py-L-Phe/BSA. These differences in the behavior of the optical antipodes are illustrated by their fluorescence decay profiles (Fig. 4). Both isomers (2 μM, air-saturated solutions, no BSA) indicate a single exponential decay with a lifetime of 105 ns, and the two data sets are indistinguishable. The fluorescence decays of the isomers, recorded in the presence of BSA (5 μM), are clearly distinguishable and indicate a biexponential behavior. The data are fit satisfactorily to a sum of two exponentials with lifetimes of 213 ns (93%) and 52 ns (7%) for the D-isomer, and the L-isomer indicated lifetimes of 188 ns (94%) and 59 ns (6%). Although these differences in the lifetimes are only minor, both isomers have lengthened lifetimes for the major component and a shorter lifetime for the minor component. These data, along with the steady-state data, establish that Py-L-Phe fluorescence is quenched by the surrounding amino acid residues of BSA via a static mechanism but not that of the D-isomer. The binding sites

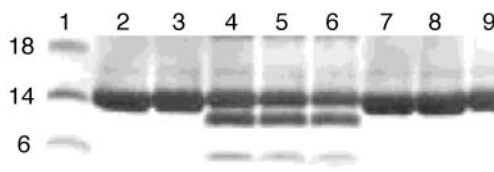

Fig. 6. Lane 1: Molecular-weight makers 18000, 14000, and 6000; lanes 2–9 contain lysozyme (15 μM), and lanes 3–6, 9 contain Py-D-Phe (15 μM). Lanes 3–6 and 8 also contain CoHA (1 mM). Lane 3 is the dark control, whereas samples in lanes 4–6 were exposed to 344-nm radiation (5, 10, and 20 min, respectively). Lane 7 contained only lysozyme that was exposed to light (344 nm, 20 min), whereas lane 8 contained lysozyme and CoHA, exposed to light (344 nm, 20 min) in the absence of Py-D-Phe. Lane 9 contained lysozyme and Py-D-Phe (irradiated at 344 nm for 20 min).

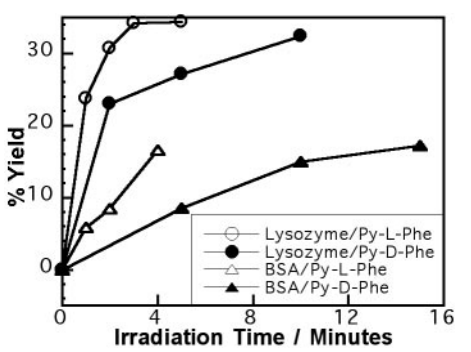

Fig. 8. Plot of photoproduct yield as a function of irradiation time for lysozyme and BSA [irradiation at 344 nm with Py-D-Phe (15 μM) or Py-L-Phe (15 μM) in the presence of CoHA (1 mM)]. The product yield reaches a maximum of ≈34% for lysozyme, whereas that for BSA reaches a maximum of ≈18%.

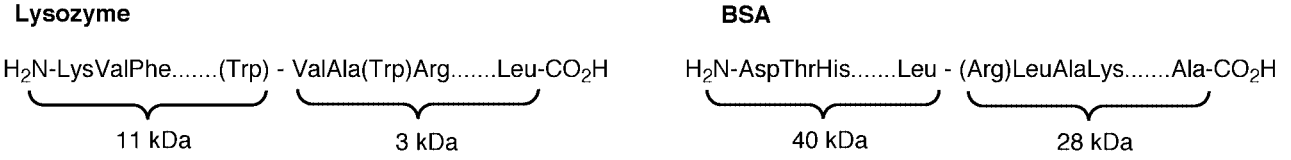

Scheme 2. The Py-D-Phe photocleavage sites on lysozyme and BSA. The cleavage sites of both enantiomers on lysozyme, as well as on BSA, are identical.

of the two isomers on BSA are distinguishable, whereas those on lysozyme are similar. These aspects are further examined in fluorescence quenching experiments, as these data provide information regarding the degree of accessibility of the pyrenyl chromophore to the solvent.

Fluorescence Quenching Studies. HexammineCo(III) chloride (CoHA) quenches Py-Phe fluorescence at diffusion controlled rates, and binding of the probe to the protein protects it from CoHA (20, 23, 24). Quenching of Py-Phe fluorescence by CoHA, however, is essential to induce protein photocleavage (19). Quantitating the differences in the accessibilities of the protein-bound isomers to CoHA, therefore, is important. The quenching constant (K_{sv}) obtained by plotting the ratio of intensity of probe fluorescence in the absence of the quencher (I_o) to the intensity in the presence of the quencher (I) as a function of CoHA concentration (Eq. **2**) (27, 28) is a measure of the probe accessibility to CoHA.

$$I_o/I = 1 + K_{sv}[Q] \qquad [2]$$

The quenching constants obtained for both the isomers, in the absence of the protein and in the presence of BSA or lysozyme, are listed in Table 1. Both isomers show quenching with equal efficiency in the absence of the protein, but in the presence of lysozyme (2 μM) the fluorescence of the L-isomer (2 μM) is quenched more efficiently than that of the D-isomer (2 μM). In contrast, addition of CoHA enhances emission from Py-D-Phe (2 μM) in the presence of BSA (2 μM), whereas that of the L-isomer (2 μM) is quenched weakly. These quenching data clearly indicate the subtle differences in the binding of the two isomers to lysozyme and BSA. On the basis of these data, one would anticipate the protein photocleavage yields to follow the order Py-L-Phe/lysozyme > Py-D-Phe/lysozyme > Py-L-Phe/BSA > Py-D-Phe/BSA. The differences in the environments of the protein-bound probes are further examined in CD experiments.

CD Spectra. The CD spectra of the two isomers, in the absence of the protein, have a mirror-image relationship, and these spectra are expected to be sensitive to the chiral environment of the probes. Addition of BSA (55 μM) to a solution of Py-L-Phe (30 μM), for example, resulted in the inversion of the sign of the major peaks in the 320- to 360-nm region when compared with the free probe (20), and a similar inversion has been observed with Py-D-Phe (Fig. 5). The CD spectra of the two isomers, in the presence of BSA, are near mirror images, but these clearly show minor differences. The isomers are likely to experience different environments on these proteins, and these may cleave the protein backbone, on photoactivation, at distinct sites. The protein-bound pyrenyl probes, therefore, are used to cleave the protein backbone to determine their cleavage location and specificity.

Protein Photocleavage Studies. On photoactivation, both isomers cleave lysozyme, as well as BSA, in the presence of CoHA with specificity, as shown in Figs. 6 and 7. Irradiation of a mixture of Py-D-Phe, CoHA and lysozyme at 344 nm resulted in two new fragments of molecular weights 11,000 and 3,000 (Fig. 6, lanes 4–6). No products are produced in the absence of light (lane 3), or CoHA (lane 9) or Py-D-Phe (lane 8). The probe, CoHA, and light, therefore, are essential for the protein photocleavage and similar results are reported for Py-L-Phe (19). Photocleavage of BSA by Py-D-Phe resulted in two fragments (Fig. 7, molecular weight ≈40,000 and ≈28,000), and these products are similar to those obtained with Py-L-Phe (Fig. 7, lanes 6 and 7). The electrophoretic mobilities of the fragments produced with both proteins, surprisingly, appear to be independent of the enantiomer used for the photocleavage. These results are in contrast to the spectral data presented above, suggesting that the cleavage specificity is robust in these systems.

Photocleavage yields, on the other hand, vary between the isomers and depend on the type of protein (Fig. 8). At early times or low conversions, the cleavage yields are in the order Py-L-Phe/lysozyme > Py-D-Phe/lysozyme > Py-L-Phe/BSA > Py-D-Phe/BSA, as predicted from the fluorescence quenching experiments. The differences diminish at high conversions, leading to the loss of chiral selectivity. The protein fragments are isolated, purified, and sequenced to examine whether the cleavage sites differ for the two isomers.

Amino Acid Sequencing Studies. The N-terminal sequencing of the 11-kDa fragment from lysozyme indicated residues LysVal-PheGly, and these correlate with the N-terminal residues of the lysozyme indicating that the 11-kDa band is at the N terminus of lysozyme. The N-terminal sequencing of the 3-kDa fragment from lysozyme indicated residues Val-Ala-Trp-Arg, which are present in the interior of lysozyme at residues 109–112, which tallies with the lysozyme segment after the cleavage of the 11-kDa fragment. The C-terminal sequencing of the 11-kDa fragment was not feasible, but the C terminus of the 3-kDa fragment indicated Leu, the C-terminal residue of lysozyme. Therefore, Py-D-Phe cleaves lysozyme at a single site between Trp-108 and Val-109 (Scheme 2), identical to that of Py-L-Phe, reported earlier (19).

Similarly, the N-terminal sequencing of the 40-kDa fragment of BSA produced by Py-D-Phe indicated residues Arg-Thr-His, and these are identical to the N terminus of BSA. The N-terminal sequencing of the 28-kDa fragment, on the other hand, indicated an internal sequence Arg-Leu-Ala (Scheme 2). From the known primary sequence of BSA, we assign the photocleavage site for Py-D-Phe at Leu-346 and Arg-347 (Scheme 2), a site identical to that of Py-L-Phe (19). The sequencing data reveal that both proteins are cleaved by Py-D-Phe with specificity (single site), and the cleavage sites are identical to that of Py-L-Phe. These results are in contrast to the differences seen in the spectral data of the optical isomers bound to BSA or lysozyme. This is a case where the physical properties of the protein-bound isomers differ, but their cleavage specificity is unaltered. To investigate the basis for the retention of the cleavage specificity, the excited state dynamics of the protein-bound probes are carried out in laser flash photolysis experiments.

Flash Photolysis Studies. Excitation of a mixture of the probe (20 μM), BSA (30 μM), and CoHA (3 mM, air-saturated solutions), with light pulses from a Nd-YAG laser (355 nm, 8-ns pulse

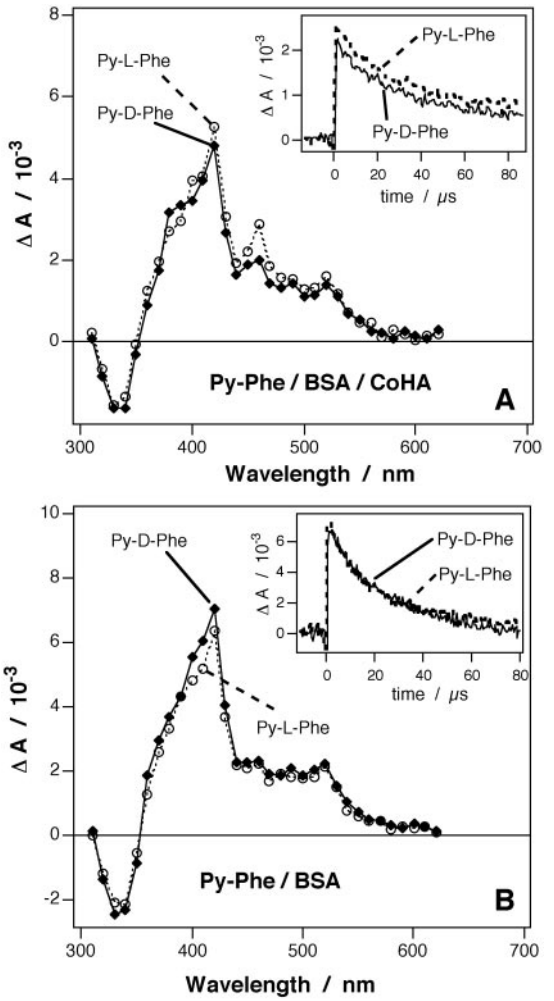

Fig. 9. Transient absorption spectra recorded 1–7 μs after laser excitation (355 nm) of air-saturated solutions of Py-D-Phe (20 μM) (open circles) and Py-L-Phe (20 μM) (closed circles), BSA (30 μM), and CoHA (3 mM) (*A*) or without CoHA (*B*) (Tris·HCl buffer, pH 7.0). *Insets* show the transient kinetics monitored at 460 nm (*A*) or 420 nm (*B*) for both optical isomers.

width) indicated the presence of several intermediates (Fig. 9*A*). Ground-state bleaching at 350 nm, where the pyrenyl probes absorb strongly, and a strong transient absorption centered around 420 nm assigned to the triplet state of the probe (19) are evident. The weak absorption at 460 nm corresponds to the pyrene cation radical (19, 29, 30), and overall the peak intensities/positions are nearly independent of the isomer examined.

The transient decay kinetics at 420 and 460 nm indicate the lifetimes of the triplet and the cation radical to be $\approx$25 μs (Fig. 9*A Inset*) and 43 μs, respectively. These values are consistent with previous reports (19, 24). In the absence of CoHA, both isomers produced the triplet as the major transient (Fig. 9*B*), and the current results are consistent with the proposed mechanism of protein photocleavage (20).

Both isomers cleave both proteins at a single site (specificity), and the differences in the cleavage efficiencies of the isomers/proteins correlate with the differences in the accessibilities of the protein-bound probe to CoHA. This observation leads to the conclusion that accessibility of the pyrenyl chromophore controls efficiency. Both proteins are cleaved at the same site, despite the differences in their binding modes. This result leads to the conclusion that both isomers access the same reactive site on the protein, irrespective of their binding modes, and the availability of specific reactive entities at the binding site controls the cleavage specificity. The size, rigidity, binding affinity, and hydrophobicity of the cation radical limit its ability to access reactive sites on the protein. Also, the availability of α hydrogens, for example, for abstraction by the cation radical depends on the local three-dimensional structure of the residues surrounding the probe, their flexibility to expose the reactive hydrogen, and the mobility of the cation radical to explore its surroundings during its limited lifetime. The data, therefore, clearly demonstrate that these features, taken together, explain the site-specific photocleavage by the chiral probes.

We thank M. Moyer and W. Burkhart of Glaxo Wellcome Laboratories, Inc., for the peptide sequencing data. C.V.K. thanks the National Science Foundation (Grant DMR-9729178), the Petroleum Research Fund (PRF no. 33821-AC4), and the Air Force Office of Scientific Research for the financial support of this work. S.J. and N.J.T. thank the National Science Foundation (Grants CHE-98-12676 and CHE-01-10655) for its generous support.

1. Suckling, C. J. (1990) *Enzyme Chemistry: Impact and Applications* (Chapman & Hall, London), 2nd Ed.
2. Westheimer, F. H., Fisher, H., Conn, E. E. & Vennesland, B. (1951) *J. Am. Chem. Soc.* **73,** 2403.
3. Kahne, D. & Still, W. C. (1988) *J. Am. Chem. Soc.* **110,** 7529–7534.
4. Rana, T. M. & Meares, C. F. (1991) *Proc. Natl. Acad. Sci. USA* **88,** 10578–10582.
5. Schepartz, A. & Cuenoud, B. (1990) *J. Am. Chem. Soc.* **112,** 3247–3249.
6. Kumar, C. V. & Buranaprapuk, A. (1997) *Angew. Chem. Int. Ed. Engl.* **36,** 2085–2087.
7. Cremo, C. R., Loo, J. A., Edmonds, C. G. & Hatlelid, K. M. (1992) *Biochemistry* **31,** 491–497.
8. Hegg, E. L. & Burstyn, J. N. (1998) *Coord. Chem. Rev.* **173,** 133–165.
9. Lehninger, A., Nelson, D. L. & Cox, M. M. (1993) *Principles of Biochemistry* (Worth, New York).
10. Kumar, C. V., Buranaprapuk, A. & Sze, H. C. (2001) *Chem. Commun*., 297–298.
11. Haque, A. & Stewart, J. T. (1998) *J. Liq. Chromatogr. Relat. Technol.* **21,** 2675–2687.
12. Allenmark, S. & Andersson, S. (1992) *Chirality* **4,** 24–29.
13. Cserhati, T. & Forgacs, E. (1999) *Int. J. Bio-Chromatogr.* **4,** 203–208,
14. Taura, T. (1996) *Inorg. Chim. Acta* **252,** 1–3.
15. Festa, C., Levi-Minzi, M. & Zandomeneghi, M. (1966) *Gazzetta Chim. Italiana* **126,** 599–603.
16. Broo, K. S., Nilsson, H., Nilsson, J. & Baltzer, L. (1998) *J. Am. Chem. Soc.* **120,** 10287–10295.
17. Kumar, C. V., Raphael, A. L. & Barton, J. K. (1986) *Biomol. Stereodyn.* **3,** 85–101.
18. Lipkowitz, K. B. (2000) *Acc. Chem. Res.* **33,** 555–562.
19. Kumar, C. V., Buranaprapuk, A., Opiteck, G. J., Moyer, M. B., Jockusch, S. & Turro, N. J. (1998) *Proc. Natl. Acad. Sci. USA* **95,** 10361–10366.
20. Kumar, C. V. & Buranaprapuk, A. (1999) *J. Am. Chem. Soc.* **121,** 4262–4270.
21. Schägger, H. & von Jagow, G. (1987) *Anal. Biochem.* **166,** 368–379.
22. McGarry, P. F., Cheh, J., Ruiz-Silva, B., Hu, S., Wang, J., Nakanishi, K. & Turro, N. J. (1996) *J. Phys. Chem.* **100,** 646–654.
23. Kumar, C. V. & Tolosa, L. M. (1993) *J. Phys. Chem.* **97,** 13914–13919.
24. Buranaprapuk, A., Kumar, C. V., Jockusch, S. & Turro, N. J. (2000) *Tetrahedron* **56,** 7019–7025.
25. Scatchard, G. (1949) *Ann. N.Y. Acad. Sci.* **51,** 660–672.
26. Tinoco, I., Jr., Sauer, K. & Wang, J. C. (1995) *in Physical Chemistry: Principles And Applications In Biological Sciences* (Prentice–Hall, Englewood Cliffs, NJ), pp. 203–208.
27. Turro, N. J. (1976) in *Modern Molecular Photochemistry* (Benjamin, New York).
28. Kumar, C. V., Barton, J. K. & Turro, N. J. (1985) *J. Am. Chem. Soc.* **107,** 5518–5523.
29. Hsiao, J. S. & Webber, S. E. (1993) *J. Phys. Chem.* **97,** 8289–8295.
30. Vala, M., Szczepanski, J., Pauzat, F., Parisel, O., Talbi, D. & Ellinger, Y. (1994) *J. Phys. Chem.* **98,** 9187–9196.